Journal of Applied Fluid Mechanics, Vol. 12, No. 2, pp. 445-459, 2019.
Available online at www.jafmonline.net, ISSN 1735-3572, EISSN 1735-3645.
DOI: 10.29252/jafm.12.02.29303

Monitoring the Performance of Centrifugal Pump under Single-Phase and Cavitation Condition: A CFD Analysis of the Number of Impeller Blades

A. Ramadhan Al-Obaidi

Department of Mechanical Engineering, Faculty of Engineering, Mustansiriyah University, Baghdad, Iraq

†*Corresponding Author Email: ahmedram@uomustansiriyah.edu.iq*

(Received June 23, 2018; accepted September 2, 2018)

ĄBSTRACT

In this current study, the transient numerical calculations using CFD are carried out under different number of impeller blades for the flow field within a centrifugal pump under single-phase and cavitation condition. Both qualitative and quantitative analyses have been carried out on all of these results in order to better understand the flow structure within a centrifugal pump under both single-phase and cavitation. Also, the investigation using different number of impeller blades relating to the static pressure, velocity magnitude and vapour volume fraction variations have been analysed. Fluctuations pressure in both time and frequency domains at the impeller and volute of the pump also investigated. As a result, the pressure and velocity were gradually increased from inlet to outlet of the pump. Pressure at the impeller outlet was higher than the pressure at other parts due to high interaction between impeller and volute tongue region. The distribution of volume fraction first occurs at the inlet eye of impeller. Furthermore, the cavitation increases as the number of impeller blades and flow rate increase. The length of the cavity was increased when low pressure at the inlet impeller (eye) decreased at Z=5 blades cavitation was affected highly at the suction of impeller compared to other number of blades particularly at high flow rate.

Keywords: Centrifugal pump; Single-Phase; Cavitation; Number of impeller blades; Pressure variations; Velocity variations.

NOMENCLATURE

BEP	Best Efficiency Point
Di	inlet impeller diameter
Do	outlet impeller diameter
H	head
NPSH	Net Positive Section Head
N1	number of vapour bubbles
Q	Flow rate
R_B	bubbles radius
R_c	mass transfer rate
ρ	fluid density
ρ_v	vapour fluid density
ρ_v	liquid fluid density

1. INTRODUCTION

Centrifugal pumps are widely used in domestic and industry applications the reasons behind that are their high efficiency, a wide range of applications, ease of maintenance and operation. The performance of the pump is measured via different standard quantities such as head, flow rate and pump rotational speed. The flow rate and head parameter are the most significant parameters in centrifugal pumps (Yunus and Cimbala, 2006). The flow field within centrifugal pump has been investigated by many researchers using CFD for example, the work done by Kim *et al.* (2012) where authors studied the effect of outlet angle of blades on performance of the centrifugal pump. The investigation was carried out under using 60 m head, 600 rpm rotating speed. The results indicated that the head increases as the outlet angle of a blade increases. In addition, efficiency decreased approximately by 0.3%. In a different study, Sidhesware and Hebbal (2013) investigated a hydraulic design of a metallic centrifugal pump volute. The authors carried out the flow simulation of a pump under different flow rates. Authors found that the pump performance (head) decreases as the flow rate increases. In addition, the pressure distribution over the suction and pressure side of blades were found to be non-uniform. Rajendran and Purushothaman (2012)

conducted a numerical investigation to analyses the flow structure in the impeller of a centrifugal pump. The pump has six blades, inlet and outlet impeller diameters of 150 mm, 280 mm. The results showed that the pressure difference from the pressure side to the suction side of the impeller blade increases from the leading edge to trailing edge. The minimum static pressure inside the impeller was located at the leading edge of the blades on the suction side. Later, the effects of centrifugal pumps' geometrical parameters investigated on pump performance was studied by Patel *et al.* (2013). They investigated the effect of impeller blades outlet angle on the performance of pump under different specific speeds. Their study has shown that the pump performance increased with the increase in the outlet blade angle. In the literature, many researchers have attempted to investigate occurrence of cavitation in centrifugal pumps using various approaches such as numerical and experimental. One of these studies done by Koné *et al.* (2011) where authors attempted to detect the centrifugal pump cavitation experimentally using visual observation through the use of a high-speed camera. Through observing visual indication of cavitation, they found that the inception of cavitation appears before the performance of the pump starts to decrease in terms of head and efficiency. Furthermore, when the flow rates and temperatures have increased the cavitation is increased as well. Another investigation carried out by Abbas (2010) who investigated cavitation within the centrifugal pump numerically. The results have shown that the formation of bubbles occurs in a lower pressure area due to the high velocity of the fluid. In addition, the cavitation happens on the surface of the blades at the leading edge. Li *et al*. (2017) studied the effect of different blade widths at the outlet, which are 11, 13 and 16mm on the pump performance and in predicting cavitation in the pump. Their results showed that as the outlet blade width increases, the pump performance gradually increases. Moreover, when the outlet blade width increases, the low static pressure region at the impeller eye also increases. Their result also shows that when the outlet blade width increases, cavitation also increases with the 11mm outlet blade width showing the best performance with little cavitation. Li *et al*. (2013) conducted another study where a numerical investigation has been carried out regarding the effect of impeller leading edge on cavitation within the centrifugal pump. In their study, they used the k-ω SST turbulence model under transient conditions. The results have shown that the pump performance drop was due to the generation of the vortex flow in the rear area of the cavity. The accuracy of the prediction for the flow regimes has been estimated to be within 5%. Chakraborty *et al*. (2011) numerically studied effects of differences blade number on performance of the pump. In this study, the pump has a design speed of 4000 rpm with various of number of blades. They used steady state simulation and moving reference frame was applied. The results have shown that the head and static pressure of the pump increase with the of blade number increases. Korkmaz, *et. al*. (2017) investigated the effects of different blade number and on performance of the deep well pump. In this work, different number of blades were used (z=5, 6, and 7). As a result, the highest performance and efficiency was at the Best Efficiency Point (BEP) of all the impellers was at z=6. Ismail *et al*. (2016) modelled the pump as turbine under different number of impeller blade using CFD. The investigation was done using centrifugal pump with the impeller diameter of 214 mm the number of the blade was varied from 5 to 8 whereas other pump geometric parameters were kept constant. The numerical results shown that the best performance and efficiency was occurred at seven blades at efficiency of 76.24%. Attempted have been made by researchers to investigate the effect of various parameters and operation conditions on performance of the centrifugal pump. After review of the literature, the following can be noted; most of the above investigations which were conducted at constant geometrical parameters of pumps and under limited operation conditions. Also, these studies are severely limited and lacked the local flow field transient analysis under different combinations of geometrical parameters of the pump for different operating conditions (with and without cavitation conditions). For instance, the local and global interrelations among pressure, velocity, vapour volume fraction distributions, and pressure fluctuations in time and frequency domains Moreover, there was a necessary for better understanding of the flow structure within the centrifugal pump as well as the effect of geometric and operational conditions on detection and diagnosis of cavitation within the pump.

2. EXPERIMENTAL SETUP FOR THE CENTRIFUGAL PUMP

Figure 1 depicts the different parts for the flow loop system of the centrifugal pump. The pump can supply water to the tank with a maximum pressure of about 10 bar. The selected flow loop system was re-circulatory and included a plastic water tank, PVC clear pipes and PVC connections components. The inlet pipe diameter of the pump was 2 inches. In addition, the outlet pipe diameter of the pump used was 1.25 inches. The tank was made of plastic with dimensions of 95×90×110cm. All pipes were transparent pipes, the reason behind that is to permit observation when the cavitation occurs.

2.1. Centrifugal Pump

Figure 2 depicts the centrifugal pump that was applied in this experimental work. The made of the applied pump is the F32/200AH series standardised centrifugal pump from Pedrollo Company. This type of pump consists of a single stage and closed type impeller. It is powered by a 4 kW, 5.5 HP, 3-phase driven motor. The current is 8.9 A and voltage ranges between 380 to 400 V. Design parameters for this pump are flow rate of up to 380 (l/min), head of about 46m at the designed flow rate, five impeller blades and design rotational speed of 2900 rpm.

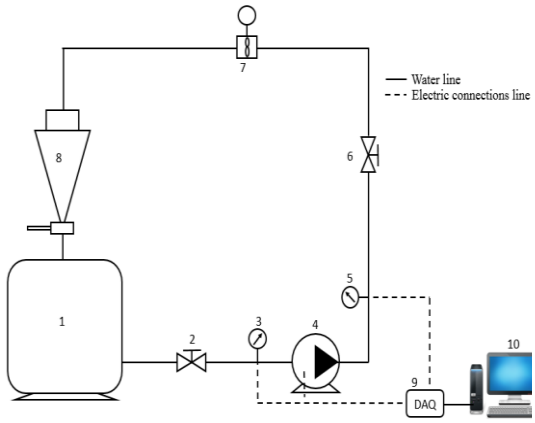

1-Water tank
2-Suction valve
3-Suction pressure transducer
4-Centrifugal pump
5-Discharge pressure transducer
6- Discharge valve
7- Water flow meter
8- Hopper
9- Data acquisition system
10- PC

Fig. 1. Components of Experimental setup for flow loop system.

Fig. 2. Centrifugal pump type F32/200AH.

3. NUMERICAL SIMULATION USING CFD TECHNIQUE

Currently, CFD analysis technique is being widely used in turbomachines industry for analysing and designing of artefacts such as turbines, compressors and various kinds of pumps. In addition, using CFD code to analyse the flow field within a centrifugal pump enables designers to have quantitative and qualitative information about likely operational behaviour of such systems. The results from numerical simulation can provide reasonably accurate information regarding to the behaviour of fluid flow in the pump. It can also be used to determine pump performance as well as to predict cavitation at the early stage. Using numerical and experimental techniques can provide detailed and effective results.

3.1. Brief Description of the Numerical Simulation Methodology for the Centrifugal Pump using CFD

The flow field within the centrifugal pump, particularly in the blade passages and volute, has an important effect on the performance of the pump. However, carrying out experiments to measure this flow field can be difficult Kim *et al*. (2012). Therefore, CFD code can be used for this purpose because it is a useful and powerful tool to study and analyse the behaviour of the flow inside the pump (Rajendran *et al.* 2012 and Wee 2011) In the present study, numerical simulation methodology was used for the centrifugal pump under single-phase and cavitation conditions. This brief methodology includes four main stages as illustrated in Fig. 3. The first stage consists of preparation of the geometry of pump parts. The second stage includes creating the meshing for each part. The third important stage in this methodology is solver setup. This stage includes providing types of domain properties, selecting the turbulence model, boundary conditions, mesh interfaces between different parts, convergence controls and numerical schemes. The final stage is to select effective parameters to monitor in the pump and then run the simulation to calculate the results, as well as collect the stored data during the post processor stage for analysing. The results can be validated with the experimental data.

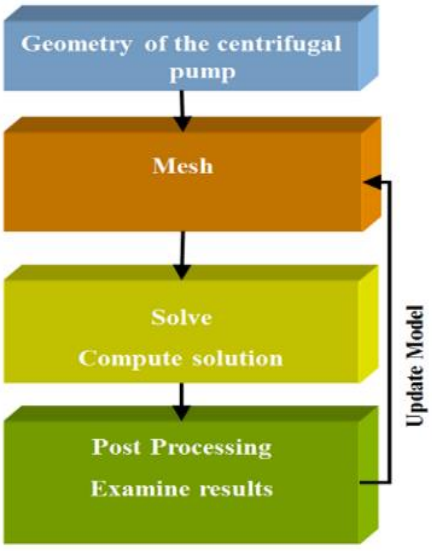

Fig. 1. Numerical methodology for the centrifugal pump using CFD code.

3.2. Pump Geometry

A numerical model of a pump in the present study was simulated with five impeller blades; the impeller was designed as a rotating part while the other parts of the geometry such as volute, inlet and outlet pipes were stationary as shown in Fig. 4. All specifications of the centrifugal pump used in this investigation are summarised in Table 1. To simulate and mimic the 3-D centrifugal pump model in a real-world scenario, the numerical model was used same specifications, dimensions, and geometrical parameters corresponding to the experimental model (F32/200AH from Pedrollo Company) in order to conduct, compare, and validate the numerical results with experimental results.

Table 1 Specifications of the centrifugal pump

Parameter	Value
Inlet diameter of the impeller (Di)	30mm
Outlet diameter of the impeller (Do)	215mm
Pump rotational speed (N)	2755 rpm
Number of blades (Z)	5
Thickness of blade	4mm
Impeller type	Backward type
Length of the inlet pipe	1m
Length of the outlet pipe	1m
Inlet blade angle	17.09º
Outlet blade angle	17.28º

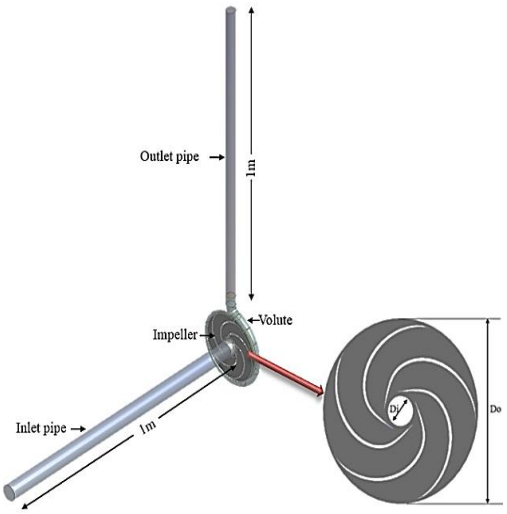

Fig. 4. Geometry of the centrifugal pump model.

3.3. Meshing of the Flow Domain

The flow domain needs to be spatially discretised into a number of small parts, each one called a mesh element, so that the fluid flow governing equations can be solved on them. This study uses an unstructured tetrahedral meshing within the flow domain because of excessive mixing and irregular geometric profile of the impeller and volute geometry. Moreover, in order to accurately capture the near-wall effects on the fluid flow, a dense mesh is generated in the near-wall regions of the flow domain. A mesh size of 1.6 mm was specified for the impeller and the volute regions, while a mesh size of 3.5 mm was used for the inlet and outlet sections. Mesh independence tests were carried out to find the optimal mesh sizing for accurate prediction of fluid flow within the domain. The mesh elements within the impeller and the volute are shown in Fig. 5.

3.4. Solving Settings in CFD Code for the Centrifugal Pump

Following sections provide the solver settings details that were used in this study.

The Physical Models Selection

For the flow diagnostics, a pressure-based solver was selected due to the fact that the density of working fluid is water, remains constant. In addition, to obtain more accurate results from the numerical simulation a transient solver was chosen for the flow diagnostics of the pump. In order to provide accurate simulation results, it is essential to choose the turbulence model suitable for the simulation calculation as the flow fields within a centrifugal pump under different operation conditions are highly turbulent and unsteady. Due to the complex separation and recirculation during the transient flow process, a reliable turbulence model selection is significant to simulate the performances more accurately. Therefore, in this study, the SST k-ω model was used in order to provide accurate results inside the centrifugal pump. The important reason behind selecting the SST k-ω model is due to this model being capable of capturing the extreme pressure gradients and the wake regions. In addition, this model can detect the variations in the flow parameters within a pump with reasonable accuracy.

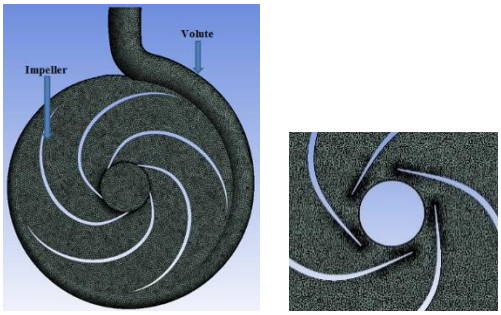

(a) (b)

Fig. 5. (a) Mesh of the centrifugal pump (b) Mesh in the impeller.

Boundary Conditions under Single-Phase Conditions

In this study, sliding mesh was used to simulate the pump under single-phase conditions. The boundary conditions for the single-phase flow simulation are set at the inlet with different velocities. The inlet velocity ranges from 0.85 to 3.1m/s, and outlet boundary condition is set as the outflow (Hua 2013 and Park 2013). The experimental data for the centrifugal pump was obtained in the lab, which was analysed in order to develop a performance prediction model for the pump.

3.5. Solver Setting for the Single-Phase Conditions

The solver settings are necessary to precisely predict the behaviour of liquid flow in the flow domain. In the current study, for the single-phase flow the SIMPLE (Semi-Implicit Method for Pressure-Linked Equations) algorithm for pressure–velocity coupling was used. Due to the use of such algorithm provides faster converges as well as it more accurate for flows within and around different geometries (Fluent, 2009). SIMPLE algorithm implements the velocity and pressure corrections to attain the pressure field and the mass conservation. The momentum equations are recorded based on the

pressure gradient collected from the previous iteration or an initial guess of pressure distribution profile to achieve velocity profile. If the initial pressure distribution does not satisfy the continuity equation, pressure and velocities are corrected until they satisfy the continuity equation (Fluent, 2009). A Green–Gauss Node based approach was adopted to compute the gradients. This approach solves a constrained minimisation problem to restructure the exact values of a linear function at a node from surrounding cell–centred values on arbitrary unstructured meshes while preserving a second-order spatial accuracy.

3.6. Interaction Between the Impeller and Volute

The flow field within a centrifugal pump is highly complicated the relative rotation between volute and impeller causes unstable flow and hence leads to the generation of more pressure fluctuations and increased level of noise and vibration. As a result, that leads to a decrease in a pump life due to fatigue which in-turn affects the pump performance (Bois, 2006). However, the knowledge regarding analysis of transient pressure fluctuations in both time and frequency domains due to interactions between the impeller and volute under different operating conditions and various geometrical parameters are still not conclusive and need more investigation. Therefore, to achieve this knowledge in this study, numerical technique by CFD code was used in order to study the effect of interactions.

In order to investigate the occurrence of cavitation within the centrifugal pump, it is necessary to calculate the performance under single-phase first and then taking these results as the basis for the initial conditions of cavitation calculation. Therefore, a detailed discussion of suitable solver settings and boundary conditions is presented in this next section under cavitation conditions.

4. CAVITATION MODEL IN THE CENTRIFUGAL PUMP

Information regarding cavitation model is provided in this section as it was used in CFD code. Such cavitation model is useful to simulate and mimic cavitation influences in two-phase flows when a mixture model is employed (ANSYS, 2013).

4.1. Cavitation Model

Characteristics of the two-phase cavitation model are:

- The cavitation model under investigation includes merely two phases and these phases are liquid-water and water-vapour.
- The model takes into consideration bubble formation (evaporation) and the collapse of bubbles (condensation) (ANSYS, 2013).

Schnerr and Sauer Model

The Schnerr-Sauer model is used to predict cavitation flow in many applications such as propellers, hydrofoils, and pumps, and it can be used in the centrifugal pump in order to detect cavitation where the Schnerr-Sauer model is defined as Liu *et al*. (2013):

$$R_c = 3\frac{\rho_v \rho_{l\propto_v}}{\rho}\frac{(1-\propto_v)}{R_B}\sqrt{\frac{2\,p_{v-}P}{3p_l}} \quad P < P_v \tag{1}$$

$$R_c = 3\frac{\rho_v \rho_{l\propto_v}}{\rho}\frac{(1-\propto_v)}{R_B}\sqrt{\frac{2\,p_{v-}P}{3p_l}} \quad P > P_v \tag{2}$$

Where, R_c is the mass transfer rate, ρ, ρ_v and ρ_l are denoted the fluid density, vapour and liquid fluid density respectively. $\propto v$ represents the vapour volume fraction. p_v, p_l are represented vapour and liquid pressures. R_B represents bubbles radius which can be calculated by using the equation:

$$R_B = \left[\frac{3\propto_v}{4\pi N1(1-\propto_v)}\right]^{1/3} \tag{3}$$

Where, N1 is the number of vapour bubbles per unit volume of fluid.

4.2. Solver Settings and Boundary Conditions for the Cavitation Model

In this study, the simulation was conducted using the Coupled algorithm for the pressure-velocity coupling and the following schemes are utilised: The coupled solver is chosen in order to solve the momentum equations that could lead to faster convergence and a more robust calculation (Li and Terwisga, 2011). The coupled solver is used to simulate the cavitation flows especially in rotating machineries such as pumps, turbines impellers and inducers. In order to correct the pressure between iterations, the PRESTO (PREssure STaggering Option) scheme is utilized (Riglin, 2012). The PRESTO can be used when the flows have highly swirling, including steep pressure gradients and the flow domains have curved boundaries such as pumps, fans, and turbines (Settings, 2006). For momentum, density, turbulent dissipation rate and turbulent kinetic energy, second order upwind schemes were used as the second order upwind provides a more accurate calculation compared to the first order upwind. In this study, the boundary condition for cavitation condition were velocity at the inlet and static pressure at the outlet Guo *et al*. (2012).

5. Analysis of the Flow Field and Performance of the Centrifugal Pump using Transient Numerical Approach

To analyse the effect of interaction between impeller and volute, numerical simulations were conducted that take into account various locations of the impeller blades relative to the volute tongue region using sliding mesh technique. Details regarding to all numerical results for the centrifugal pump, model reliability including mesh independence test, time independence test, and validation will be represented in the next sub sections.

5.1. Mesh Independence Test

Testing the mesh independence is important because meshing can lead to less or more accurate outcomes. In this study, three meshes consisting of 1.25 million, 2.5 million, and 5 million mesh elements were selected as displayed in Table 2. The outcomes of these three cases showed that the change in the head predicted within the centrifugal pump is less than 3.14% amongst the three meshes under consideration.

Table 2 Results of mesh independence of the centrifugal pump

No.	No. of elements	Head
		(m)
1	1.25 million	37.53
2	2.5 million	38.75
3	5 million	38.84

5.2. Time Steps Independence Test

Time step independence can lead to less or more accurate outcomes of the Computational Fluid Dynamics. This study includes the usage of three different time steps. The outcomes of time steps are summarised in the Table 3 shows that the variance in the head within the centrifugal pump is less than 1.11% between the three-time steps under consideration. Therefore, the time step with $3.0248*10^{-4}$sec was selected for further analysis.

Table 3 Results of Time step independence of the pump

No.	Time steps	Head
	(s)	(m)
1	$6.04960*10^{-5}$	38.01
2	$1.81488*10^{-4}$	38.44
3	$3.02480*10^{-4}$	38.75

5.3. Validation

The validation of the outcomes is considered as one of the most significant steps when conducting numerical studies. In other words, it means that the results gained from the numerical simulations are compared with experimental findings to verify accurately that the numerical model symbolises the physical model of the actual system. Thus, the entire geometric, flow and solver-related parameters and variables become vital in validation studies. In the present study, the experimental data for the centrifugal pump was provided by experimental investigations to validate the model used in the CFD. Figure 6 depicts the variation in (a) head, (b) power and (c) efficiency for both numerical and experimental results. It can be seen that there is a good agreement between CFD and the experimental results in this figure. From previous analysis, it can be seen that both results match closely with each other and this agreement confirms that the CFD results are reasonable. It can be concluded from the above findings that the numerical analysis is reasonably well validated.

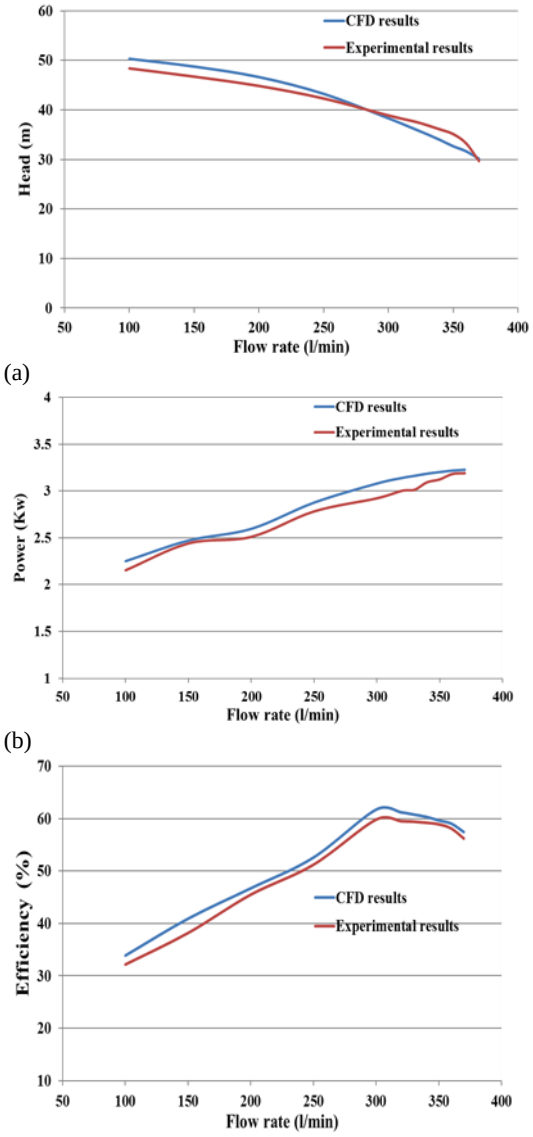

Fig. 6. Validation of the numerical and experimental (a) head, (b) power and (c) efficiency of the pump.

Figure 7 depicts the relationship between the head of the pump and NPSH. The net positive suction head represents the difference between the liquid's absolute pressure in the system and the vapour pressure of the liquid at a given temperature. It shows the head drop of the pump under flow rate of 300 (l/min) corresponding to points A, B, C, D, E, F and G. In this figure, the curve of head-NPSH can be divided into three parts. The first part shows when the NPSH is equal to between 6.89m and 9m, an inception of cavitation occurs in this region. The second part displays the occurrence of the development of cavitation when the NPSH is equal to 5.87m corresponding to head drop of about 4.36%. The

third and final part illustrates the full development of cavitation when the NPSH is equal to 3.83 m with a head drop of 10.84%. Furthermore, when the NPSH decreases, the cavitation on the suction side of the pump begins to develop.

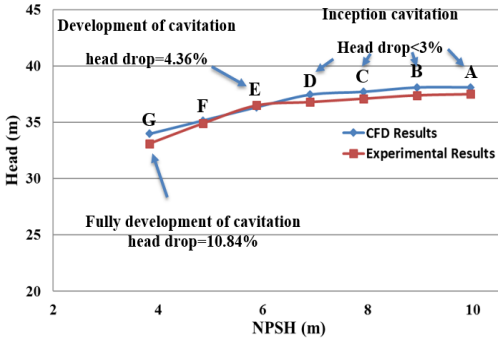

Fig. 7. NPSH for the cavitation characteristics prediction curve of the pump.

To analyse the effect of the number of impeller blades on the performance of the pump under single-phase and cavitation conditions, three different number of impeller blades 3, 4, and 5 have been selected for the analysis purpose. The next section represents the results obtained from the calculation of the different number of impeller blades. In this study, two types of numerical simulation were carried out to investigate the characteristics of the pump performance and visualise the flow field within a centrifugal pump. The first category was a numerical simulation under single-phase operating conditions. The second was to simulate cavitation under different operating conditions.

5.4. Analyses of Inner Flow in Single-Phase Condition (Pressure and Velocity Variations)

Figure 8 depicts the static pressure variations within the centrifugal pump corresponding to operating conditions were flow rate of 300 (l/min), inlet and outlet impeller diameters of 35 mm and 220 mm and N=2755 rpm and Z=3, 4, and 5 blades. It can be noticed that the pressure is increased gradually from the inlet to the outlet of the impeller. Under these operating conditions, the static pressure of the blade's pressure surface is higher than the suction surface. The lower pressure inside the impeller is positioned at the suction surface of the blade. The high-pressure region for Z=4 is higher than for Z=3 by 6.7%, and for Z=5 is higher than Z=4 by about 3.57%. Based on the above analysis, it can be seen that when the number of impeller blades increase the static pressure also increases.

On further analysing for the flow structure within the centrifugal pump, Fig. 9 depicts the velocity magnitude variations at the middle section of the pump. It can be seen that the velocity increases from inlet to exit of the impeller at the design flow rate through the passages between the blades. In addition, it can be seen that the high-velocity region for Z=4 is higher than for Z=3 by 4.65%. Furthermore, velocity for Z=5 is slightly higher for Z=4 by 2.27%.

Many monitoring points are set in the volute and impeller in order to analyse the pressure fluctuation in the pump under different number of blades as shown in the following section.

5.5. Analyses of Pressure Fluctuations Characteristics in the Centrifugal Pump

The internal flow field in pumps are complex and there are several reasons behind their complexity. Firstly, it is due to the high interaction between fluid and impeller blades as well as the interaction between the rotor part (impeller) and stationary part (volute) especially at volute tongue region. Secondly, it is due to the effect of turbulence and the complex unsteady effects within the pump. Thirdly, the most important reason is the occurrence of cavitation. For Further, investigations for pressure fluctuations analyses in the impeller and volute at different monitoring points will be discussed in the next section.

5.6. Monitoring Points on the Impeller and Volute

Many monitoring points are set in the impeller and volute of the pump to investigate and develop comprehensive understanding of the pressure fluctuations within the centrifugal pump under various number of blades and different operational conditions. For this purpose, there are 15 points that were marked in the volute, including 6 points inside the volute, which are set at every 60^o, 3 points are set close to the tongue region and in addition, 6 points are set at the outlet of the volute, a further 8 points are set in the impeller. The monitoring points for volute are referred to as VP1 to VP12 and for impeller are called IP1 to IP8. Figure 10Fig. 1 depicts the distribution of the monitoring points within a centrifugal pump.

6.7. Time Domain Analysis (TDA) in the Pump

Figure 11 (a) depicts the pressure fluctuations for 12 monitoring points on the volute with a flow rate of 300 (l/min), do=220 mm, di=35 mm, N=2755 rpm and Z=3, 4, and 5 blades. It is obvious that the pressure fluctuations at the monitoring points are increased near or close to the tongue region then decreased when they are located far from the tongue area. In addition, the highest-pressure fluctuations are at the area near the tongue and in the outlet pipe of the volute regions. The higher-pressure fluctuation in the volute at for Z=4 is higher than that for Z=3 by about 6.34%. Furthermore, the pressure fluctuation in the volute at for Z=5 is slightly higher than for Z=4 by 2.67%.

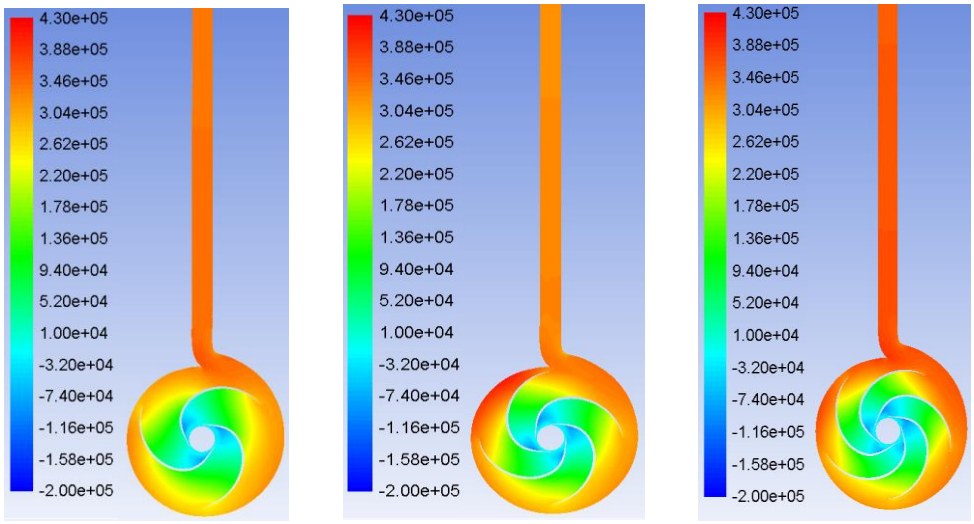

Z=3 Z=4 Z=5

Fig. 8. Static pressure variations of the pump under different number of blades.

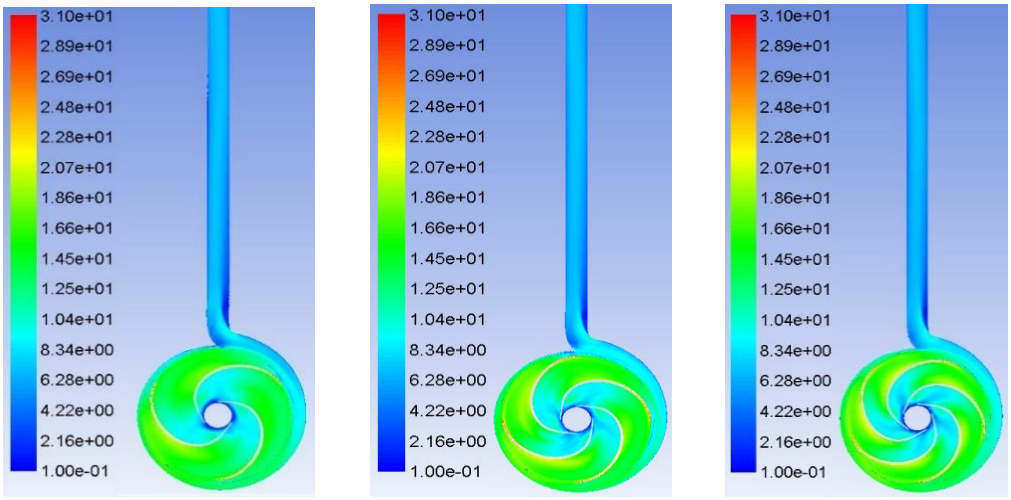

Z=3 Z=4 Z=5

Fig. 9. Velocity magnitude variations of the pump under different number of blades.

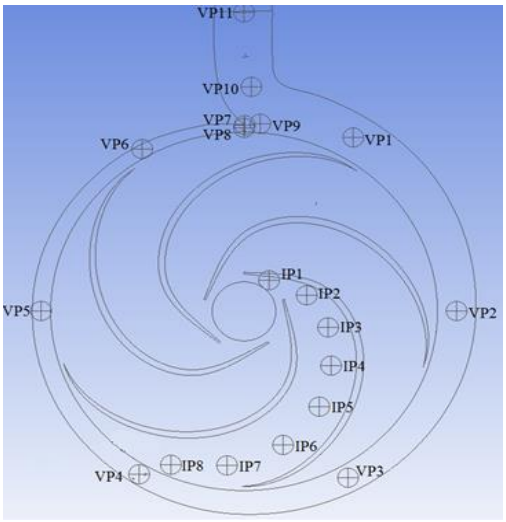

Fig. 10. Distribution of monitoring point's positions in the centrifugal pump.

Figure 11 (b) depicts the pressure fluctuations along the angular location within the impeller under different number of blades. It can be seen that pressure fluctuations at the inlet of an impeller are low and the pressure fluctuations are increased when the distance along the radius of the impeller is increased, with the maximum value found at the outlet of the impeller diameter. The maximum pressure fluctuations are at points IP7 and IP8. This is due to increased interaction between the impeller and volute, which have high effects on the impeller flow close to this particular area. This figure also displays that the static pressure has maximum values within the tongue region. In addition, pressure fluctuation in the impeller at IP8 for Z=4 is slightly higher than that for Z=3 by about 2.01%. Pressure fluctuation in the impeller at IP8 for Z=5 is slightly higher than for Z=4 by 4.71%.

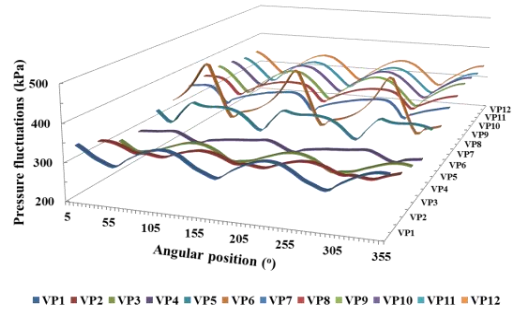

(a)Z=3

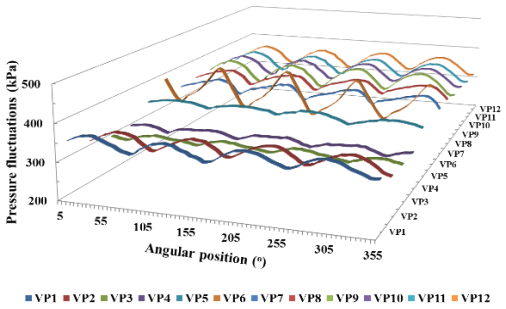

(a)Z=4

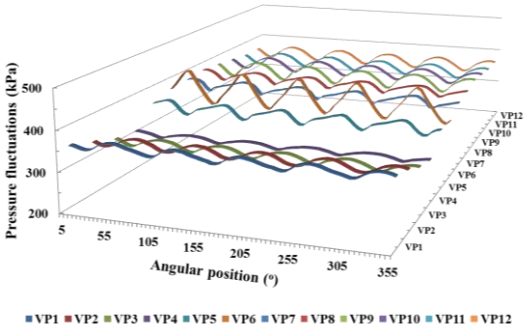

(a) Z=5

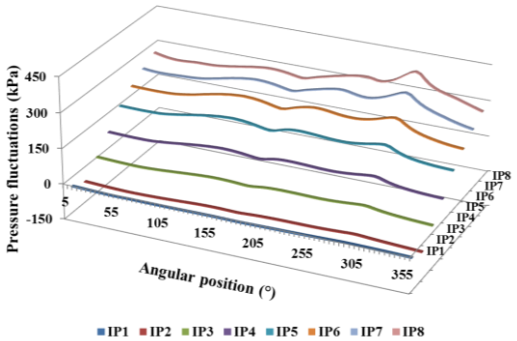

(b)Z=3

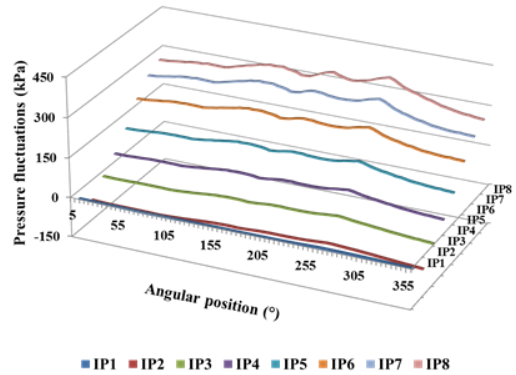

(b) Z=4

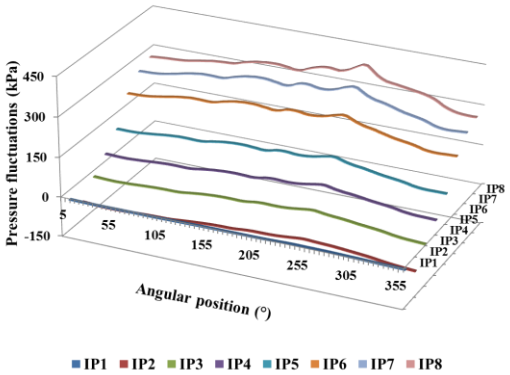

(b) Z=5

Fig. 11. (a) Pressure fluctuations around the volute and (b) at the impeller of the pump under different number of blades.

5.7. Frequency Domain Analysis (FDA) in the Pump

Figure 12 (a) depicts the amplitudes of pressure fluctuations against frequencies for the 12 monitoring points around the volute for these cases under consideration. It can be seen that in the volute the maximum pressure fluctuation amplitude for all monitoring points is at a Blade Passing Frequency (BPF). However, the maximum pressure fluctuation amplitudes were at monitoring points are VP6 and VP9. The reason behind that is due to the location of these points being near the tongue region. In addition, at point PV4, the pressure fluctuation amplitude reaches the lowest point due to its location, far away from the volute tongue area. It can be observed that the maximum pressure fluctuation amplitude in the volute at points VP6 for Z=4 was lower than for Z=3 by 45.25%, and for Z=5 is lower than for Z=4 by 15.58%. This happened due to the distance between blade to blade for Z=3 was higher than Z=4. Hence, that leads to the value of peak-to-peak of pressure fluctuations for Z=3 being higher than Z=4 by 22.86%, and for Z=4 being higher than Z=5 by 23.15%.

Figure 12 (b) depicts obvious variations in the amplitudes of pressure fluctuations with frequencies for eight monitoring points at the impeller under different number of blades. The first maximum amplitude of pressure fluctuations for entire points

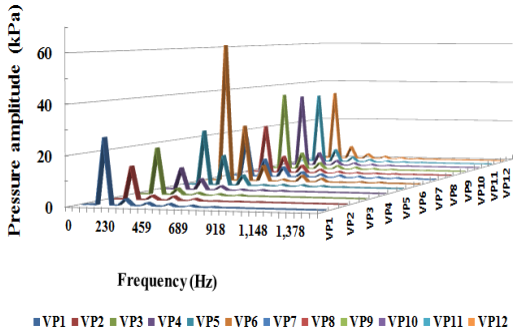

(a)Z=3

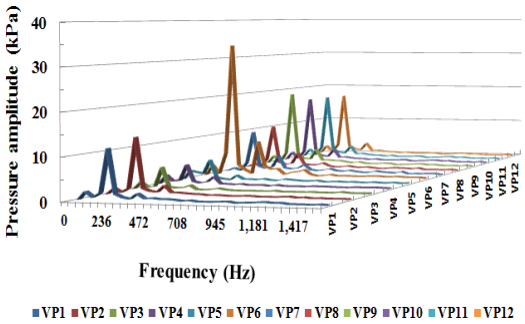

(a)Z=4

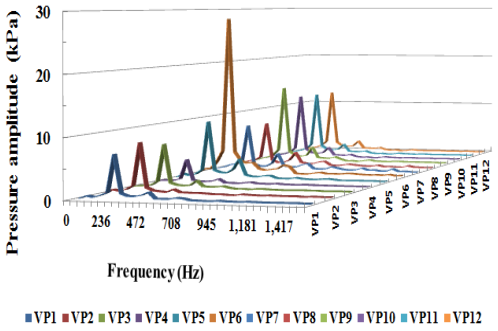

(a) Z=5

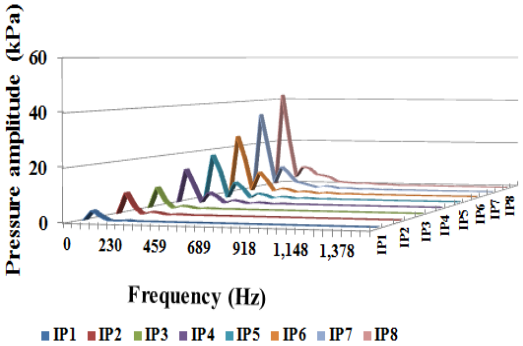

(a) Z=3

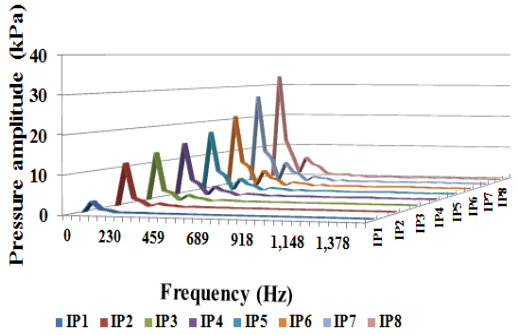

(b) Z=4

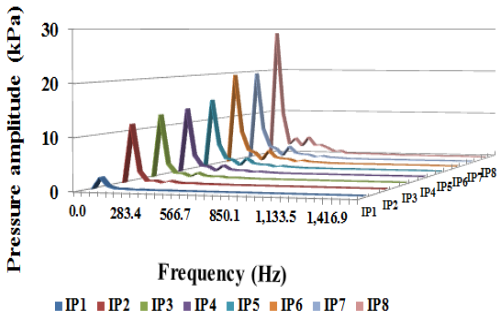

(b) Z=5

Fig. 12. (a) Frequency spectra around the volute and (b) in the impeller under different number of blades.

Table 4 Maximum amplitude of static pressure fluctuations under different number of blades

Z=3								
Frequency	Maximum amplitude of pressure fluctuations for 8 monitoring points at the impeller (kPa)							
Hz	IP1	IP2	IP3	IP4	IP5	IP6	IP7	IP8
45.92	3.80	8.33	8.33	13.84	18.19	25.00	33.81	42.19
Z=4								
Hz	IP1	IP2	IP3	IP4	IP5	IP6	IP7	IP8
45.92	2.87	11.42	13.10	14.71	17.07	21.05	26.70	32.83
Z=5								
Hz	IP1	IP2	IP3	IP4	IP5	IP6	IP7	IP8
47.23	2.28	11.53	12.67	13.28	14.55	19.60	19.60	28.96

is at rotational frequency (Rf). Table 4 summaries the amplitudes of pressure fluctuation at (Rf) in the impeller. It can be clearly seen that the amplitudes of pressure fluctuations increase as the distance along the radius of the impeller is increased. The pressure fluctuation amplitudes in the impeller are

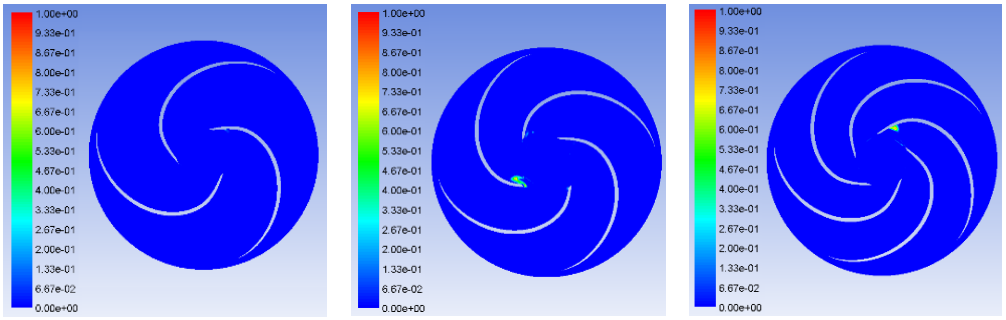

Fig. 13. Volume fraction distributions for the pump under different number of blades.

lower than in the volute. Additionally, it can be observed that the maximum amplitude pressure fluctuation on the impeller at point IP8 for Z=4 is lower than that for Z=3 by around 22.20%, and the maximum pressure fluctuation amplitude at the impeller for Z=4 is higher than for Z=5 by 11.798%. This is because of the (max. pressure – min. pressure) value for the peak-to-peak for Z=3 is also higher than that for Z=4 and Z=5. Based on the findings in this work, different investigations on the global and local flow fields for static pressure and fluctuations pressure in time and frequency domains were carried out. Also, comparative investigations to estimate the effects of various number of blades under single-phase and cavitation at transient flow conditions were carried out in order to better understanding the effect of number of blades on all of these parameters.

5.8. Analyses of Cavitation Characteristics in the Impeller

Figure 13 depicts the transient simulation of cavitation in the centrifugal pump having a flow rate of 300 (l/min), do=220 mm, di=35 mm, N=2755 rpm, and Z=3, 4, and 5 blades. It can be seen that there is no cavitation in case Z=3, and the vapour volume fractions zone within the impeller of the pump for Z=4, and 5 models are slightly higher than that of Z=3, due to these cases operate under design flow rate of 300 (l/min).

For comparison purposes between the above models, Figs. 14 (a) and (b) depict the instantaneous head of the aforementioned cases under single-phase and cavitation conditions. It can be clearly seen that for the model that has Z=5, the average head under single-phase and cavitation conditions are considerably higher than for the other two models Z=4 and Z=3 by 11.09% and 2.64%, and under cavitation condition by 11.04% and 3.16% respectively. In comparison, between the models when Z=4 and Z=5, the maximum instantaneous head for Z=5 is seen to be higher than that of Z=4. The results showed that as the number of impeller blades increases, the head of the centrifugal pump increases. Table 5 summarises the boundary conditions and NPSH values for different cavitation cases under various number of blades and flow rates.

Table 5 Boundary conditions and NPSH values for different cavitation cases

Cases		Boundary conditions		
Q	Z	Inlet	Outlet	NPSH
(l/min)	(-)	Velocity (m/s)	Pressure (kPa)	(m)
300	3	2.546	314.276	4.82
330	3	2.801	308.824	4.32
350	3	2.970	270.417	4.18
300	4	2.546	327.965	5.24
330	4	2.801	311.309	4.87
350	4	2.970	284.313	4.32
300	5	2.546	352.555	5.72
330	5	2.801	333.012	5.52
350	5	2.970	304.796	4.87

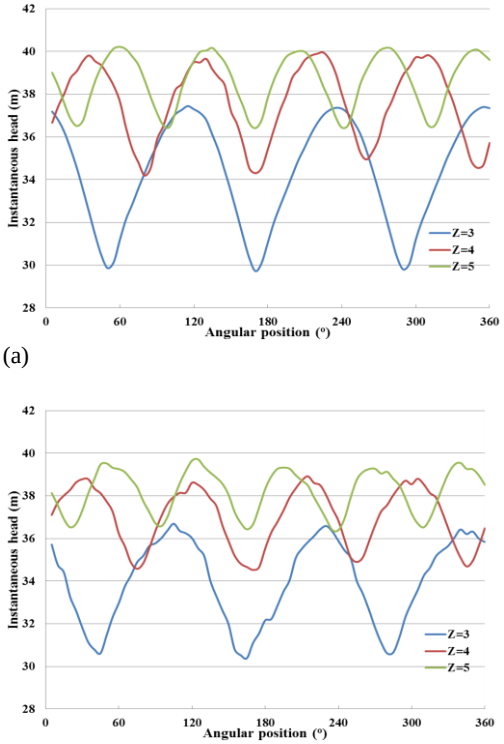

Fig. 14. Instantaneous head variations of centrifugal pump models having different number of blades (Z) under (a) single-phase and (b) cavitation conditions.

From Figure 15 it can be seen that when the flow rate, pump rotational speed, inlet and outlet impeller diameters are kept constant and number of impeller blades (Z) is increased, the average head of the pump increases under both single-phase and cavitation conditions. Also, there is a slight difference between the head for both single-phase and cavitation under different number of impeller blades. The head for the single-phase is slightly higher than the head for the cavitation condition by 1.02, 1.54, and 1.01% for when Z=3, 4, and 5 respectively. All of these cases under investigation were conducted under design flow rate of 300(l/min) and the level and severity of cavitation was found to be relatively small under this flow rate. In addition, the results showed that as the number of blades increases, the head of the pump increases. The maximum performance of the centrifugal pump corresponds with the optimum value of the number of blades (Z), which in the current study is five blades.

Further quantifying the performance of the pump, Table 6 provides the statistical analysis results of the instantaneous head such as the maximum, minimum, average, and (max–min) amplitude under single-phase and cavitation condition at different number of blades.

Table 6 Statistical analysis results of the instantaneous head under single-phase and cavitation conditions at different number of blades

Single-phase			
Head (m)	Z=3	Z=4	Z=5
Average	34.31	37.57	38.59
Minimum	29.72	34.19	36.41
Maximum	37.44	39.94	40.21
Max - Min	7.72	5.75	3.79
Cavitation condition			
Head (m)	Z=3	Z=4	Z=5
Average	33.96	36.99	38.20
Minimum	30.38	34.52	36.39
Maximum	36.69	38.91	39.71
Max - Min	6.309	4.392	3.315

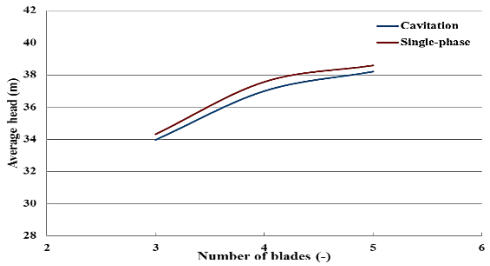

Fig. 15. Effect of number of impeller blades on performance of the centrifugal pump under single-phase and cavitation conditions.

Under different number of impeller blades, the low-pressure region occurs at the inlet eye of the impeller, particularly at the suction side of blades near the leading edges. Also, when the blade number increases, it leads to the region of low-pressure area increases, causing cavitation to increase due to the decrease in the low-pressure region at this particular area. Therefore, the number of impeller blade has a high influence on the pump characteristics and cavitation within the centrifugal pump.

5.9. Detection of Cavitation under Different Number of Impeller Blades and Flow Rates

Figure 16 depicts the vapour volume fraction variations under various flow rates namely 300, 330, and 350 (l/min). The number of impeller blades that have been used are 3, 4, and 5, inlet and outlet impeller diameters used are di=35 mm, do=220 mm, and N=2775 rpm was the speed of operation. The numerical results found that the occurrence of cavitation changes with the number of impeller blades and flow rates. It can be seen that at 300 (l/min) flow rate, there was no occurrence of cavitation at Z=3, but small cavitation occurs when the number of impeller blades goes up to Z=5. In addition, cavitation initiates from the leading edge of the impeller and the magnitude of the cavitation increases as the number of impeller blades and flow rate increase. In addition, the length of the cavity is increased when low pressure at the inlet impeller (eye) decreases. The possible reason behind that is due to an increase in the number of impeller blades and flow rate, leading to pressure at the eye of impeller continually decreases. In addition, at Z=5 blades, cavitation was affected highly at the suction of the impeller compared to the number of blades at 4 and 3, especially at high flow rate. Furthermore, based on the above analysis, the numerical results showed that the number of blades and flow rates have a high effect on cavitation within a pump, particularly at the eye of impeller region.

The numerical results showed that as the number of impeller blade increases, static pressure also increases, hence, the pump head increases. As well, under different number of impeller blades, the low-pressure region occurs at the inlet eye of the impeller, particularly at the suction side of blades near the leading edges. In addition, when the blade number increases, it leads to the region of low-pressure area increasing, causing cavitation to increase due to the decrease in the low-pressure region at this particular area. Therefore, the number of impeller blade has a high influence on the pump characteristics and cavitation in the pump.

6. CONCLUSION

Detailed flow diagnostics within the centrifugal under single-phase and cavitation conditions and effect of different impeller number of impeller blades showed the following results:

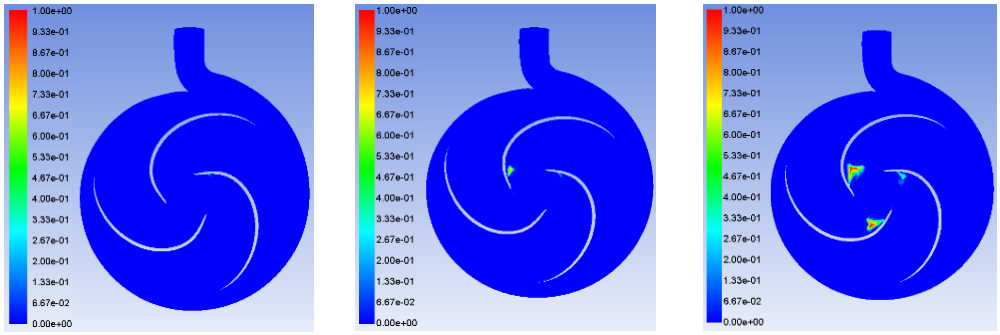

Fig. 16. Volume fraction distributions for the centrifugal pump under different number of impeller blades and flow rates.

1- The pressure gradually increases from inlet to outlet impeller of the pump. Pressure at the impeller outlet is higher than the pressure at other parts of the impeller when the impeller rotates close to the tongue region of the volute.

2- The velocity gradually increases from the inlet to outlet impeller of the pump also. The high velocity occurs at the outlet of the impeller close to the tongue region.

3- The interaction between impeller and volute tongue region is actually according to the relative position of the impeller blades with respect to tongue region.

4- There are two dominant frequencies, the rotational frequency (Rf), and Blade Passing Frequency (BPF) and their related harmonics.

5- The numerical results showed that the distribution of volume fraction within a pump first occurs at the inlet eye of the impeller close to the leading blade.

6- The results show that as the number of impeller blades increases, the occurrence of cavitation increases.

7- CFD can be a useful tool to predict and analyse the outcome characteristics and performance of the centrifugal pump with reasonable accuracy under single-phase and cavitation conditions.

8- The detailed investigations of cavitation characteristics were presented in this study in order to provide useful information and guidance regarding the inception and development of cavitation within the centrifugal pump under different number of blades and operation conditions.

ACKNOWLEDGEMENTS

The author would like to thank Mustansiriyah University (HYPERLINK "http://www. uomustansiriyah.edu.iq" www.uomustansiriyah. edu.iq) Baghdad – Iraq for its support in the present work. The author also would like to gratefully acknowledge the University of Huddersfield (UK) due to the pump geometry and numerical data were carried out when the author was studied his PhD degree in this University.

REFERENCES

Abbas, M. K. (2010). Cavitation in centrifugal pumps. *Diyala Journal of Engineering Sciences*, 170-180.

ANSYS (2013). *ANSYS Fluent Theory Guide Release 15.0*. Published in the U.S.A.

Bois, G. (2006). *Introduction to design and analysis of high speed pumps*. Ecole Nationale Superieure D'arts Et Metiers Lille, France.

Chakraborty, S. and K. M. Pandey (2011). Numerical Studies on Effects of Blade Number Variationson Performance of Centrifugal Pumps at 4000 RPM. *International Journal of Engineering and Technology* 3(4), 410.

Cui, B., C. Wang, Z. Zhu and Y. Jin (2013). Influence of blade outlet angle on performance of low-specific-speed centrifugal pump. *Journal of Thermal Science* 22(2), 117-122..

Cui, B., D. Chen, C. Wang, Z. Zhu, Y. Jin and Y. Jin (2013). Research on performance of centrifugal pump with different-type open impeller. *Journal of Thermal Science* 22(6), 586-591.

Fluent, A. (2009). *12.0 Theory Guide. Ansys Inc*, 5(5). Certified to ISO 9001:2008.

Guo, X., Z. Zhu, B. Cui and Y. Li (2012). Analysis of Cavitation Performance of Inducers in Centrifugal pumps. INTECH.

Hua, T., L. Yi and Z. Yu-Liang (2013). Numerical analysis of a prototype centrifugal pump delivering solid-liquid two-phase flow. *Journal of Applied Sciences* 13, 3416-3420.

Ismail, M. A. I., A. K. Othman, H. Zen and M. S. Misran (2016). CFD Modelling of pump as turbine with various number of blade for microhydro system. *Journal of Applied Science & Process Engineering* 3(1).

Kim, J. H., K. T. Oh, K. B. Pyun, C. K. Kim, Y. S. Choi and J. Y. Yoon (2012). Design optimization of a centrifugal pump impeller and volute using computational fluid dynamics. *IOP Conference Series: Earth and Environmental Science* (Vol. 15, No. 3, 032025). IOP Publishing.

Koné, W. M., B. Dro, K. Yao and K. Kamanzi (2011). Detection of Cavitation in Centrifugal Pumps. *Australian Journal of Basic and Applied Sciences* 5(11), 1260-1267.

Korkmaz, E., M. Gölcü and C. Kurbanoğlu (2017). Effects of blade discharge angle, blade number and splitter blade length on deep well pump performance. *Journal of Applied Fluid Mechanics* 10(2), 529-540.

Li, W., X. Zhao, W. Li, W. Shi, L. Ji and L. Zhou (2017). Numerical Prediction and Performance Experiment in an Engine Cooling Water Pump with Different Blade Outlet Widths. *Mathematical Problems in Engineering*.

Li, X., S. Yuan, Z. Pan, J. Yuan and Y. Fu (2013). Numerical simulation of leading edge cavitation within the whole flow passage of a centrifugal pump. *Science China Technological Sciences* 56(9), 2156-2162.

Li, Z. and T. Terwisga (2011). On the capability of multiphase RANS codes to predict cavitation erosion. In *Second International Symposium on Marine Propulsors*.

Liu, H. L., D. X. Liu, Y. Wang, X. F. Wu and J. Wang (2013). Application of modified κ-ω model to predicting cavitating flow in centrifugal pump. *Water Science and Engineering* 6(3), 331-339.

Park, K. (2013). *Optimal design of a micro vertical axis wind turbine for sustainable urban environment*. Doctoral dissertation, University of Huddersfield, UK.

Patel, M. G. and A. V. Doshi (2013). Effect of impeller blade exit angle on the performance of centrifugal pump. Int J. *Emerging Technology and Advanced Engineering* 3(1), 91-99.

Rajendran, S. and D. K. Purushothaman (2012). Analysis of a centrifugal pump impeller using ANSYS-CFX. *International Journal of Engineering Research & Technology* 1(3).

Riglin, J. D. (2012). *Cavitation Study of a Microhydro Turbine*. Theses and Dissertations. Paper 1134. Lehigh University, USA.

Settings, S. (2006). *Introductory FLUENT training v 6.3* Fluent User Services Center, ANSYS. Inc. Proprietary. Fluent User Services Center.

Sidhesware, R. and O. D. Hebbal (2013). Validation Of Hydraulic Design Of A Metallic Volute Centrifugal Pump. *International Journal of Engineering Research & Technology* 2.

Wee, C. K. (2011). *Unsteady Flow in Centrifugal Pump at Design and Off-Design Conditions* (Doctoral dissertation). National University of Singapore, Singapore.

Yunus, A. C., and J. M. Cimbala (2006). *Fluid mechanics fundamentals and applications*. International Edition, McGraw Hill Publication, 185201. 1221 Avenue of the Americas, New York, NY 10020, USA.